

Optimization of High-Performance Blue Organic Light-Emitting Diodes Containing Tetraphenylsilane Molecular Glass Materials

Li-Hsin Chan,[†] Rong-Ho Lee,[‡] Chia-Fen Hsieh,[‡] Hsiu-Chih Yeh,[†] and Chin-Ti Chen^{*,†}

Contribution from the Institute of Chemistry, Academia Sinica, Taipei, Taiwan 11529, ROC, and Opto-Electronics & Systems Laboratory, Industrial Technology Research Institute, Chutung, Hsinchu, Taiwan 310, ROC

Received January 3, 2002

Abstract: Molecular glass material (4-(5-(4-(diphenylamino)phenyl)-2-oxadiazolyl)phenyl)triphenylsilane ($\text{Ph}_3\text{Si}(\text{PhTPAOXD})$) was used as the blue light-emitting material in the fabrication of high-performance organic light-emitting diodes (OLEDs). In the optimization of performance, five types of OLEDs were constructed from $\text{Ph}_3\text{Si}(\text{PhTPAOXD})$: device I, ITO/NPB/ $\text{Ph}_3\text{Si}(\text{PhTPAOXD})/\text{Alq}_3/\text{Mg:Ag}$, where NPB and Alq_3 are 1,4-bis(1-naphylphenylamino)biphenyl and tris(8-hydroxyquinoline)aluminum, respectively; device II, ITO/NPB/ $\text{Ph}_3\text{Si}(\text{PhTPAOXD})/\text{TPBI}/\text{Mg:Ag}$, where TPBI is 1,3,5-tris(*N*-phenylbenzimidazol-2-yl)benzene; device III, ITO/ $\text{Ph}_2\text{Si}(\text{Ph}(\text{NPA})_2)_2/\text{Ph}_3\text{Si}(\text{PhTPAOXD})/\text{TPBI}/\text{Mg:Ag}$, where $\text{Ph}_2\text{Si}(\text{Ph}(\text{NPA})_2)_2$ is bis(3,5-bis-(1-naphylphenylamino)phenyl)-diphenylsilane, a newly synthesized tetraphenylsilane-containing triarylamine as hole-transporting material; device IV, ITO/ $\text{Ph}_2\text{Si}(\text{Ph}(\text{NPA})_2)_2/\text{NPB}/\text{Ph}_3\text{Si}(\text{PhTPAOXD})/\text{TPBI}/\text{Mg:Ag}$; device V, ITO/ $\text{CuPc}/\text{NPB}/\text{Ph}_3\text{Si}(\text{PhTPAOXD})/\text{Alq}_3/\text{LiF}/\text{Al}$, where CuPc is Cu(II) phthalocyanine. Device performances, including blue color purity, electroluminescence (EL) intensity, current density, and efficiency, vary drastically by changing the device thickness (100–600 Å of the light-emitting layer) and materials for hole-transporting layer (NPB and/or $\text{Ph}_2\text{Si}(\text{Ph}(\text{NPA})_2)_2$) or electron-transporting material (Alq_3 or TPBI). One of the superior OLEDs is device IV, showing maximum EL near 19 000 cd/m² with relatively low current density of 674 mA/cm² (or near 3000 cd/m² at 100 mA/cm²) and high external quantum efficiency of 2.4% (1.1 lm/W or 3.1 cd/A). The device possesses good blue color purity with EL emission maximum ($\lambda_{\text{max}}^{\text{EL}}$) at 460 nm, corresponding to (0.16, 0.18) of blue color chromaticity on CIE coordinates. In addition, the device is reasonably stable and sustains heating over 100 °C with no loss of luminance on the basis of the annealing data for device V. Formation of the exciplex at the interface of NPB and $\text{Ph}_3\text{Si}(\text{PhTPAOXD})$ layers is verified by EL and photoluminescence (PL) spectra studies on the devices with a combination of different charge transporting materials. The EL due to the exciplex ($\lambda_{\text{max}}^{\text{EL}}$ at 490–510 nm) can be properly avoided by using a 200 Å layer of $\text{Ph}_3\text{Si}(\text{PhTPAOXD})$ in device I, which limits the charge-recombination zone away from the interface area.

Introduction

Organic light-emitting diodes (OLEDs) are now considered the only flat-panel technology with the potential to pose a realistic challenge to liquid crystal displays (LCDs), which dominate the ever-increasing market for last few decades.¹ There are already companies in production of monochromic OLEDs (for display panel of mobile phone and car stereo) using either small molecule or polymer materials.² Full-color OLED display is one of the next inroads into the flat-panel display market. Among several issues, one of the major concerns in the

fabrication of full-color OLEDs is the equal performance of the three primary colors of red, green, and blue.³ Due to the large band gap energy, blue light-emitting materials have a low affinity for the electron from the cathode in OLED devices. Therefore, the performance of blue emitters is usually inferior to that of green or red emitters and it is not satisfactory. Specifically, the color purity and stability require improvement for blue OLEDs.^{3,4}

Organosilicon-containing OLED materials have been known for sometime. Polysilane polymers have been used as hole-transporting materials for the fabrication of multilayer OLEDs.⁵ Polysilanes are also known for their uncommon ultraviolet or near-ultraviolet light-emitting performance.⁶ As a substituent,

* Corresponding author. E-mail: cchen@chem.sinica.edu.tw.

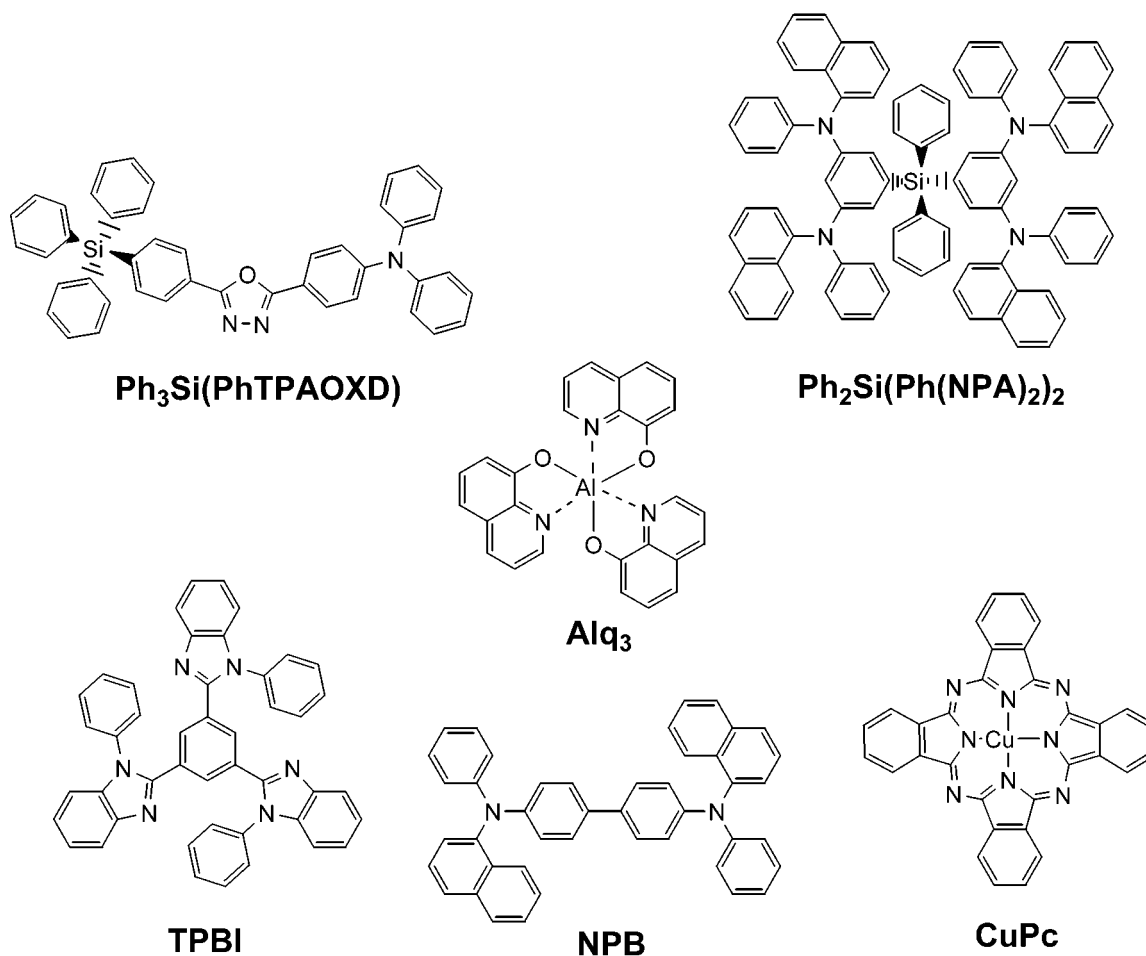
[†] Academia Sinica.

[‡] Industrial Technology Research Institute.

- (1) (a) Kelly, S. M. *Flat Panel Displays: Advanced Organic Materials*; Royal Society of Chemistry: Cambridge, U.K., 2000; p 1. (b) Tullo, A. H. *Chem. Eng. News* **2000**, 78 (June 26), 20. (c) Tullo, A. H. *Chem. Eng. News* **2001**, 79 (Nov 19), 49.
- (2) (a) Dixon, R. *Compd Semicond.* **1999**, 5 (Nov/Dec), 43. (b) Johnstone, B. *Technol. Rev.* **2001**, 104 (3), 80.

(3) Sato, Y. *Semicond. Semimet.* **2000**, 64, 209.

(4) (a) Rajeswaren, G.; Ito, M.; Boroson, M.; Barry, S.; Hatwar, T. K.; Kahen, K. B.; Yoneda, Y.; Yokoyama, R.; Yamada, T.; Komiyama, N.; Kanno, H.; Takahashi, H. *SID 2000 Dig.* **2000**, 40.1, 1. (b) O'Connor, S. J. M.; Towns, C. R.; O'Dell, R.; Burroughes, J. H. *Proc. SPIE-Int. Soc. Opt. Eng.* **2001**, 4105, 9.

Chart 1. Chemical Structures of Ph₃Si(PhTPAOXD), Ph₃Si(Ph(NPA)₂)₂, Alq₃, TPBI, NPB, and CuPc

the alkylsilyl group is helpful in solubility and widening the band gap of poly(phenylenevinylene) (PPV) type π -conjugated light-emitting polymers.⁷ Recently, silole (silacyclopentadiene) derivatives have shown high electron mobility as well as green-blue light-emitting ability.⁸ Silyl-contained phenylene-vinylene derivatives either as small molecules or polymers have been proven to be effective as a blue light-emitting materials in the fabrication of high brightness blue OLEDs.⁹

More recently, we communicated a blue OLED with a strong emission of electroluminescence ($\lambda_{\text{max}}^{\text{EL}}$) at 460 nm, corresponding to color coordinates of (0.17, 0.17),¹⁰ inside the region of pure blue on a CIE (Commission Internationale de l'Eclairage) 1931 chromaticity diagram.¹¹ The blue electroluminescence (EL) can reach a maximum intensity as high as 20 130 cd/cm², surpassing most of known small molecule-based bright blue OLEDs, which have maximum luminance in the range of 6000–19 000 cd/cm² with similar color purity.^{8c,9c,d,12} The blue emitter of the OLED is Ph₃Si(PhTPAOXD), a (diphenylamino)oxadiazole-substituted tetraphenylsilane compound (Chart 1). Ph₃Si(PhTPAOXD) has proven to be an authentic molecular glass material with an on-set glass transition temperature (T_g) around 85 °C.¹¹ There is no clear evidence that those previously known molecule-based bright blue emitters, except Ph₃Si(PhTPAOXD),

- (5) (a) Kido, J.; Nagai, K.; Okamoto, Y.; Skotheim, T. *Chem. Lett.* **1991**, 1267. (b) Suzuki, H.; Meyer, H.; Simmerer, J.; Yang, J.; Haarer, D. *Adv. Mater.* **1993**, *5*, 743. (c) Suzuki, H.; Meyer, H.; Hoshino, S.; Haarer, D. *J. Appl. Phys.* **1995**, *78*, 2684. (d) Suzuki, H.; Hoshino, S. *J. Appl. Phys.* **1996**, *79*, 858. (e) Cimrová, V.; Neher, D.; Remmers, M.; Kminek, I. *Adv. Mater.* **1998**, *10*, 676.
- (6) (a) Xu, Y.; Fujino, T.; Naito, H.; Oka, K.; Dohmaru, T. *Chem. Lett.* **1998**, 299. (b) Suzuki, H.; Hoshino, S.; Yuan, C.-H.; Fujiki, M.; Toyoda, S. *Thin Solid Films* **1998**, *331*, 64. (c) Hoshino, S.; Ebata, K.; Furukawa, K. *J. Appl. Phys.* **2000**, *87*, 1968. (d) Hoshino, S.; Furukawa, K.; Ebata, K.; Yuan, C.-H.; Suzuki, H. *J. Appl. Phys.* **2000**, *87*, 2892.
- (7) (a) Höger, S.; McNamara, J. J.; Schrickler, S.; Wudl, F. *Chem. Mater.* **1994**, *6*, 171. (b) Zhang, C.; Höger, S.; Pakbaz, P.; Wudl, F.; Heeger, A. J. *J. Electron. Mater.* **1994**, *23*, 453. (c) Hwang, D. H.; Shim, H. K.; Lee, J. I.; Lee, K. S. *J. Chem. Soc., Chem. Commun.* **1994**, 2461. (d) Hwang, D. H.; Kim, S. T.; Shim, H. K.; Holmes, A. B.; Moratti, S. C.; Friend, R. H. *Chem. Commun.* **1996**, 2241. (e) Kim, S. T.; Hung, D.-H.; Li, X. C.; Grunter, J.; Friend, R. H.; Holmes, A. B.; Shim, H. K. *Adv. Mater.* **1996**, *8*, 979. (f) Chuah, B. S.; Hwang, D.-H.; Kim, S. T.; Moratti, S. C.; Holmes, A. B.; de Mello, J. C.; Friend, R. H. *Synth. Met.* **1997**, *91*, 279.
- (8) (a) Tamao, K.; Uchida, M.; Izumizawa, T.; Furukawa, K.; Yamaguchi, S. *J. Am. Chem. Soc.* **1996**, *118*, 11974. (b) Yamaguchi, S.; Endo, T.; Uchida, M.; Izumizawa, T.; Furukawa, K.; Tamao, K. *Chem.—Eur. J.* **2000**, *6*, 1683. (c) Uchida, M.; Izumizawa, T.; Nakano, T.; Yamaguchi, S.; Tamao, K.; Furukawa, K. *Chem. Mater.* **2001**, *13*, 2680. (d) Murata, H.; Malliaras, G. G.; Uchida, M.; Shen, Y.; Kafafi, Z. H. *Chem. Phys. Lett.* **2001**, *339*, 161. (e) Luo, J.; Xie, Z.; Lam, J. W. Y.; Cheng, L.; Chen, H.; Qiu, C.; Kwok, H. S.; Zhan, X.; Liu, Y.; Zhu, D.; Tang, B. Z. *Chem. Commun.* **2001**, 1740.
- (9) (a) Brouwer, J. J.; Krasnikov, V. V.; Hilberer, A.; Hadziioannou, G. *Adv. Mater.* **1996**, *8*, 935. (b) Garten, F.; Hilberer, C.; Cacialli, F.; Esselink, E.; van Dam, Y.; Schlatmann, B.; Friend, R. H.; Klappwijk, T. M.; Hadziioannou, G. *Adv. Mater.* **1997**, *9*, 127. (c) Gao, Z.; Lee, C. S.; Bello, I. Lee, S. T.; Chen, R.-M.; Luh, T.-Y.; Shi, J.; Tang, C. W. *Appl. Phys. Lett.* **1999**, *74*, 865. (11 000 cd/m², 470 nm, silyl-substituted ter-(phenylene-vinylene) derivative, dopant) (d) Wu, C.-C.; Chen, C.-W.; Lin, Y.-T.; Yu, H.-L.; Hsu, J.-H.; Luh, T.-Y. **2001**, *79*, 3023.
- (10) For comparison purpose, the CIE coordinates of blue luminance for the National Television System Committee (NTSC) is (0.14, 0.06), for Standard CRT Phosphors is (0.16, 0.07) (Society of Motion Picture and Television Engineers, SMPTE-C) or (0.15, 0.06) (European Broadcasting Union, EBU), for Sharp LCD is (0.15, 0.11), and for Kodak OLED display is (0.15, 0.15): Cropper, A. D.; Cok, R. S.; Feldman, R. D. *Proc. SPIE-Int. Soc. Opt. Eng.* **2001**, *4105*, 18.
- (11) (a) Chan, L.-H.; Yeh, H.-C.; Chen, C.-T. *Adv. Mater.* **2001**, *13*, 1637. (b) Chan, L.-H.; Yeh, H.-C.; Chen, C.-T. *Proc. SPIE-Int. Soc. Opt. Eng.* **2002**, *4464*, 265.

have a stable glass state. A considerable amount of evidence indicates that an amorphous thin film (in OLED devices) with high T_g s is less vulnerable to heat and hence more stable.¹³ Here, we want to report the temperature stability, which is crucial in practical application, of the blue OLED based on amorphous $\text{Ph}_3\text{Si}(\text{PhTPAOXD})$. In addition, despite the respectable EL properties (color purity, luminescence intensity), the device showed relatively low efficiency (1.7%) and high current density ($>1200 \text{ mA/cm}^2$) was required to reach high level of blue luminescence. High current density has an adverse effect on device's operation lifetime and should be avoided for high-performance OLEDs. The results in optimizing the device for high-performance blue OLED will be described in this report. Finally, in our previous communication,^{11a} we observed little or no emission from the exciplex, which is presumably formed at the interface between charge (hole or electron) transporting and $\text{Ph}_3\text{Si}(\text{PhTPAOXD})$ layers. This is rather unusual for short-wavelength blue OLED devices. Exciplexes usually contribute an EL emission with lower energy and hence impair the color purity of the blue OLEDs. This report includes a detail investigation in understanding the nature of the exciplex in the device, which also reveals the possible failure mechanism of the blue OLEDs reported here.

Experimental Section

General Methods. ^1H and ^{13}C NMR spectra were recorded on a Bruker AMX-400 MHz or AC-300 MHz Fourier transform spectrometer at room temperature. Elemental analyses (on a Perkin-Elmer 2400 CHN elemental analyzer) and fast atom bombardment (FAB) mass spectra (on a VG Analytical 11-250J) were recorded by the Elemental Analyses and Mass Spectroscopic Laboratory in-house service of the Institute of Chemistry, Academia Sinica. Photoluminescence (PL) spectra and powder X-ray diffraction (PXRD) spectra were recorded on a Hitachi F-4500 fluorescence spectrophotometer and Siemens D5000 X-ray diffractometer, respectively. Melting points (T_m), glass transition temperatures (T_g), and crystallization temperatures (T_c) of respective compounds were measured by differential scanning calorimetry (DSC) under nitrogen atmosphere using a Perkin-Elmer DSC-6 differential

scanning calorimeter. Redox potentials of the compounds were determined by cyclic voltammetry (CV) using a BAS 100B electrochemical analyzer with a scanning rate at 100 mV/s. The interested compound was dissolved in deoxygenated dry CH_2Cl_2 with 0.1 M tetrabutylammonium perchlorate as the electrolyte. We used a platinum working electrode and a saturated nonaqueous Ag/AgNO_3 referenced electrode. Ferrocene was used for potential calibration (all reported potentials are referenced against Ag/Ag^+) and for reversibility criteria.

Materials. The synthesis and characterization of $\text{Ph}_3\text{Si}(\text{PhTPAOXD})$ have been reported in our previous communication.^{11a} $\text{Cu}(\text{II})$ phthalocyanine (CuPc) was purchased from Eastman Kodak. Electron-transporting material 2,2',2''-(1,3,5-phenylene)tris[1-phenyl-1*H*-benzimidazole] (TPBI) was prepared from benzene-1,3,5-tricarbonyl chloride and *N*-phenyl-1,2-phenylenediamine, followed by dehydration at a temperature $>200 \text{ }^\circ\text{C}$ under reduced pressure.¹⁴ Both tris(8-hydroxyquinoline)aluminum (Alq_3) and 1,4-bis(1-naphylphenylamino)biphenyl (NPB) were prepared via published methods. Other chemicals were commercially available and used as received. $\text{Ph}_3\text{Si}(\text{PhTPAOXD})$, CuPc , TPBI, Alq_3 , NPB, and $\text{Ph}_3\text{Si}(\text{Ph}(\text{NPA})_2)_2$ were all subjected to gradient sublimation prior to use. Previously unknown triarylamine $\text{Ph}_3\text{Si}(\text{Ph}(\text{NPA})_2)_2$ is also a tetraphenylsilane-containing species. The synthesis and characterization of $\text{Ph}_3\text{Si}(\text{Ph}(\text{NPA})_2)_2$ and its precursor compound in the synthesis are reported here.

Bis(4-(3,5-dibromophenyl)diphenylsilane. *n*-Butyllithium (1.6 M in hexane, 25.0 mL, 40 mmol) was added dropwise to a dry ether solution (400 mL) containing 1,3,5-tribromobenzene (12.8 g, 40.0 mmol) under nitrogen atmosphere at $-78 \text{ }^\circ\text{C}$. The reaction solution was further stirred for 2 h. Dichlorodiphenylsilane (4.33 mL, 20 mmol) was then added dropwise to the solution. The solution was stirred and gradually allowed to warm up to room temperature in 5 h, and then the reaction was quenched with water (300 mL). The mixture was extracted with ether. The product as a white solid was isolated by flash column chromatography (silica gel, hexanes as eluent). Yield: 50% (6.6 g). ^1H NMR (400 MHz, CDCl_3): δ (ppm) 7.75 (t, 2H, $J = 1.8 \text{ Hz}$), 7.50 (d, 4H, $J = 1.8 \text{ Hz}$), 7.39–7.5 (m, 10H). ^{13}C NMR (400 MHz, CDCl_3): δ (ppm) 138.6, 137.0, 136.2, 135.7, 130.9, 130.6, 128.4, 123.6.

Bis(3,5-bis(1-naphthylphenylamino)phenyl)diphenylsilane ($\text{Ph}_2\text{Si}(\text{Ph}(\text{NPA})_2)_2$). Bis(4-(3,5-dibromophenyl)diphenylsilane (6.52 g, 10.0 mmol) and *N*-phenyl-1-naphthylamine (8.8 g, 40 mmol) were dissolved in dry xylenes (60 mL). Sodium *tert*-butoxide (4.8 g, 48 mmol) was first added to the xylenes solution under nitrogen atmosphere. After the solution mixture was stirred for 5 min, palladium acetate (22.5 mg, 0.1 mmol) and tri-*tert*-butylphosphine (0.1 mL, 48 mmol) were then added to the solution. The resulting mixture was stirred for 5 h at refluxing temperature under the protection of nitrogen atmosphere. After being cooled to ambient temperature, the reaction was quenched with excess water (100 mL). The mixture was extracted with dichloromethane. The organic phase was washed with water and dried. The solvent was removed, and the residual was subjected for flash column chromatography (silica gel, dichloromethane/hexanes, 3/7). The product was isolated as an off-white powder and became a pale yellow glassy solid after sublimation. Yield: 79% (9.64 g). ^1H NMR (400 MHz, CD_2Cl_2): δ (ppm) 7.84 (d, 4H, $J = 8.2 \text{ Hz}$), 7.75 (d, 4H, $J = 8.4 \text{ Hz}$), 7.66 (d, 4H, $J = 8.3 \text{ Hz}$), 7.42–7.47 (m, 4H), 7.25–7.35 (m, 8H), 7.08–7.13 (m, 6H), 6.95–7.02 (m, 8H), 6.86–6.92 (m, 8H), 6.75–6.82 (m, 12H), 6.60 (t, 2H, $J = 2.2 \text{ Hz}$), 6.54 (d, 4H, $J = 2.2 \text{ Hz}$). ^{13}C NMR (400 MHz, CDCl_3): δ (ppm) 148.9, 148.5, 143.8, 136.2, 135.9, 135.7, 134.4, 131.5, 129.6, 129.4, 129.0, 128.0, 127.4, 126.9, 126.8, 126.6, 124.8, 122.7, 122.3, 116.4. FAB-MS: calcd MW, 1205.56; $m/e = 1205$ (M^+). Anal. Found (calcd) for $\text{C}_{88}\text{H}_{64}\text{N}_4\text{Si}$ ($\text{Ph}_2\text{Si}(\text{Ph}(\text{NPA})_2)_2$): C, 87.90 (87.67); H, 5.25 (5.35); N, 4.55 (4.65).

Fabrication and Characterization of Light-Emitting Diodes. OLED devices were fabricated by thermal vacuum deposition. The

- (12) For blue OLEDs with maximum brightness in the range of 6000–19 000 cd/m^2 , organic emitters are the following: (a) Hosokawa, C.; Higashi, H.; Nakamura, H.; Kusumoto, T. *Appl. Phys. Lett.* **1995**, *67*, 3853 (10 000 cd/m^2 , 475 nm). (b) Tamoto, N.; Adachi, C.; Nagai, K. *Chem. Mater.* **1997**, *9*, 1077 (19 000 cd/m^2 , 490 nm). (c) Tao, Y.-T.; Balasubramanian, E.; Danel, A.; Tomasik, P. *Appl. Phys. Lett.* **2000**, *77*, 933 (11 200 cd/m^2 , 460 nm (0.18, 0.17)). (d) Tao, Y.-T.; Balasubramanian, E.; Danel, A.; Wisla, A.; Tomasik, P. *J. Mater. Chem.* **2001**, *11*, 768 (13 300 cd/m^2 , 455 nm (0.19, 0.16)). Values for metal chelates or complex emitters are the following: (e) Tao, X. T.; Suzuki, H.; Wada, T.; Miyata, S.; Sasabe, H. *J. Am. Chem. Soc.* **1999**, *121*, 9447 (6900 cd/m^2 , 470 nm). (f) Leung, L. M.; Lo, W. Y.; So, S. K.; Lee, K. M.; Choi, W. K. *J. Am. Chem. Soc.* **2000**, *122*, 5640 (14 070 cd/m^2 , 485 nm). (g) Tokito, S.; Noda, K.; Tanaka, H.; Taga, Y.; Tsutsui, T. *Synth. Met.* **2000**, *111–112*, 393 (11 000 cd/m^2 , 450 nm (0.17, 0.16)). (h) Liu, Y.; Guo, J.; Feng, J.; Zhang, H.; Li, Y.; Wang, Y. *Appl. Phys. Lett.* **2001**, *78*, 2300 (15 000 cd/m^2 , 460 nm). (i) Im, W.-B.; Hwang, H.-K.; Lee, J.-G.; Han, K.; Kim, Y. *Appl. Phys. Lett.* **2001**, *79*, 1387 (14 000 cd/m^2 , 447 nm (0.15, 0.11)). Values of maximum luminance are included in unit of cd/m^2 at the end of each reference. Numbers with nanometers as units are reported $\lambda_{\text{max}}^{\text{EL}}$ of the device; fractional numbers in parentheses denote reported CIE 1931 chromaticity coordinates.
- (13) For a general review, see the following: (a) Shirota, Y. *J. Mater. Chem.* **2000**, *10*, 1 and references therein. For arylamine-based hole-transporting materials, see the following: (b) Tolito, S.; Tanaka, H.; Noda, K.; Okada, A.; Taga, Y. *Appl. Phys. Lett.* **1997**, *70*, 1929. (c) O'Brien, D. F.; Burrows, P. E.; Forrest, S. R.; Konne, B. E.; Loy, D. E.; Thompson, M. E. *Adv. Mater.* **1998**, *10*, 1108. (d) Konne, B. E.; Loy, D. E.; Thompson, M. E. *Chem. Mater.* **1998**, *10*, 2235. (e) Steuber, F.; Staudigel, J.; Stössel, M.; Simmerer, J.; Winnacker, A.; Spreitzer, H.; Weissörtel, F.; Salbeck, J. *Adv. Mater.* **2000**, *12*, 130. For spiro-based light-emitting materials or oxadiazole-based electron-transporting materials, see the following: (f) Salbeck, J.; Yu, N.; Bauer, J.; Weissörtel, F.; Bestgen, H. *Synth. Met.* **1997**, *91*, 209.

- (14) Shi, J.; Tang, C. W.; Chen, C. H. U.S. Patent No. 5645948, 1997.

Table 1. Characteristics of Devices I–V^a

device	x	max luminance (cd/m ²)	current density at max luminance ^b (mA/cm ²)	luminance at current densities of 100 and 10 mA/cm ² (cd/m ²)	max device efficiency (%, lm/W, cd/A)	$\lambda_{\max}^{\text{EL}}$ (nm)	CIE 1931 chromaticity (x, y)
I	600	490	65		1.1, 0.2, 0.8	437	(0.17, 0.08)
I	500	1 095	134	780, 36	0.8, 0.2, 0.8	437	(0.19, 0.15)
I	400	3 581	238	1502, 29	0.9, 0.5, 1.0	437	(0.21, 0.24)
I	300	21 255	758	3427, 217	1.8, 1.1, 3.4	476	(0.18, 0.28)
I	200	20 130	1213	1978, 160	1.7, 0.9, 2.0	460	(0.17, 0.17)
I	100	18 500	862	2191, 86	1.3, 0.8, 2.4	467	(0.20, 0.27)
II	400	3 166	318	1020, 87	1.2, 0.3, 1.1	444	(0.17, 0.12)
II	300	11 134	600	2093, 186	1.7, 0.8, 2.1	457	(0.18, 0.19)
II	200	13 438	854	2052, 198	1.7, 0.9, 2.1	460	(0.16, 0.17)
II	100	15 386	1060	2065, 212	1.6, 1.2, 2.1	457	(0.17, 0.20)
III		21 750	456	5913, 580	3.0, 3.1, 6.1	487	(0.21, 0.33)
IV		18 813	674	2960, 205	2.4, 1.1, 3.1	460	(0.16, 0.18)
V		10 260	277	3500, 335	-, 1.1, 3.9	489	(0.15, 0.26)

^a Device I: ITO/NPB(400 Å)/Ph₃Si(PhTPAOXD)(x Å)/Alq₃(400 Å)/Mg:Ag. Device II: ITO/NPB(400 Å)/Ph₃Si(PhTPAOXD)(x Å)/TPBI(400 Å)/Mg:Ag. Device III: ITO/Ph₂Si(Ph(NPA)₂)₂(400 Å)/Ph₃Si(PhTPAOXD)(200 Å)/Alq₃(400 Å)/Mg:Ag. Device IV: ITO/Ph₂Si(Ph(NPA)₂)₂(400 Å)/NPB(50 Å)/Ph₃Si(PhTPAOXD)(200 Å)/Alq₃(400 Å)/Mg:Ag. Device V: ITO/CuPc(125 Å)/NPB(400 Å)/Ph₃Si(PhTPAOXD)(200 Å)/Alq₃(400 Å)/LiF(10 Å)/Al. ^b All devices showed maximum luminance at a driving voltage of 15 V.

substrate was an indium–tin–oxide (ITO) coated glass (Merck Display Technology, Taiwan) with a sheet resistance of <50 Ω/sq. The pretreatment of ITO includes a routine chemical cleaning using detergent and alcohol in sequence, followed by oxygen plasma cleaning. The thermal evaporation of organic materials was carried out using ULVAC Cryogenics at a chamber pressure of 10^{−6} Torr. The thickness of each layer was determined by quartz thickness monitor (ULVAC CRTM-6000). The cathode of Mg_{0.9}Ag_{0.1} alloy was deposited (50 nm) by coevaporation and followed by a thick layer of silver capping layer. The effective size of the emitting diode was 3.14 mm². Current–voltage–luminance (*I–V–L*) measurements were made simultaneously using a Keithley 2400 source meter and a Newport 1835C optical meter equipped with a Newport 818-ST silicon photodiode, respectively. The measurements for devices were made at room temperature under ambient condition, except those temperature-dependent studies. The EL was measured using the fluorescence spectrophotometer by blocking the incident light.

For devices with LiF/Al as cathode material, the conditions in device fabrication or measurement were somewhat different from those of devices with Mg:Ag as cathode materials. The substrate was an ITO-coated glass (Apply Film) with a sheet resistance of <20 Ω/sq. The cathode of LiF/Al was prepared first thermally deposited a LiF thin film (5–10 Å) followed by the deposition of Al metal (2000 Å) as the top layer. The thickness of each layer material was determined similarly as before. The effective size of the emitting diode was 2 mm². The devices subjected for annealing studies were all encapsulated with glass slides, which were attached to the device by UV-cured epoxy glue. The current–voltage characteristics were measured on a programmable electrometer having current and voltage sources (Keithley). For devices with LiF/Al as cathode, the luminance was measured with a luminance meter BM-8 (TOPCON).

Results and Discussion

We have fabricated five types of OLED devices. The configuration of these five devices is described under Table 1. These devices can be categorized in two types, devices with MgAg as cathode material (devices I–IV) and devices with LiF/Al as cathode material (device V). In addition to the optimization of device performance, device V was fabricated for the usage of temperature stability test. In the process of optimization of device performance, we have also searched for reliable evidence of the plausible exciplex associated with Ph₃Si(PhTPAOXD) and charge-transporting material used in device fabrication. Also, the temperature stability test of device V provides us

insightful information about the failure mechanism of OLED based on molecular materials.

A. Characteristics of Device I. Previously we observed that device ITO/NPB (400 Å)/Ph₃Si(PhTPAOXD) (x Å)/Alq₃ (400 Å)/Mg:Ag with x = 200 Å could emit pure blue EL exceeding intensity of 20 000 cd/m². However, the relatively low efficiency and high current density required for the device prompted us to search for a new device with better performance. Without changing materials, the most straightforward approach is to vary the thickness (x) of the light-emitting layer of the device. In addition to 200 Å, devices with 600, 500, 400, 300, and 100 Å were fabricated. Table 1 summarizes performance characteristics, including maximum luminance, current density at maximum luminance, luminance at 100 mA/cm² of current density, device efficiency, $\lambda_{\max}^{\text{EL}}$, and color coordinates of CIE 1931 chromaticity diagram, of device I's. We notice that device I with a 300 Å layer of Ph₃Si(PhTPAOXD) shows better performances on luminance (>21 000 cd/m² and >3400 cd/m² at current density of 100 mA/cm²), current density (<760 mA/cm² at maximum luminance), and efficiency (1.8%, 1.1 lm/W, and 3.4 cd/A). However, a device with a 200 Å layer of Ph₃Si(PhTPAOXD) still should be considered a better one among device I's, if both the purity of blue color and the intensity of EL emission are major concerns. From Table 1, the performance of the devices varies widely following the different thickness of the Ph₃Si(PhTPAOXD) layer. Then, it is not so surprising to see that EL spectra of the devices also change dramatically (Figure 1). It is evident that the EL spectra of the device are highly dependent on the thickness of the light-emitting layer.

When the radiometric EL spectra are converted into a chromaticity on a CIE (Commission Internationale de l'Éclairage) 1931 diagram, coordinates value (x and y) also shift significantly between dark purple blue, blue, and greenish blue regions. Device I with 300 Å layer of Ph₃Si(PhTPAOXD) is not a satisfactory OLED considering blue color purity, and so are not devices with 100 and 400 Å layers of Ph₃Si(PhTPAOXD).

Some of the EL spectra shown in Figure 1 seem to be complicated and irrational, particularly for devices with 100 and 300 Å layers of Ph₃Si(PhTPAOXD), although some of them can be easily identified. We have previously proven that the center of EL emission band of Ph₃Si(PhTPAOXD) itself is

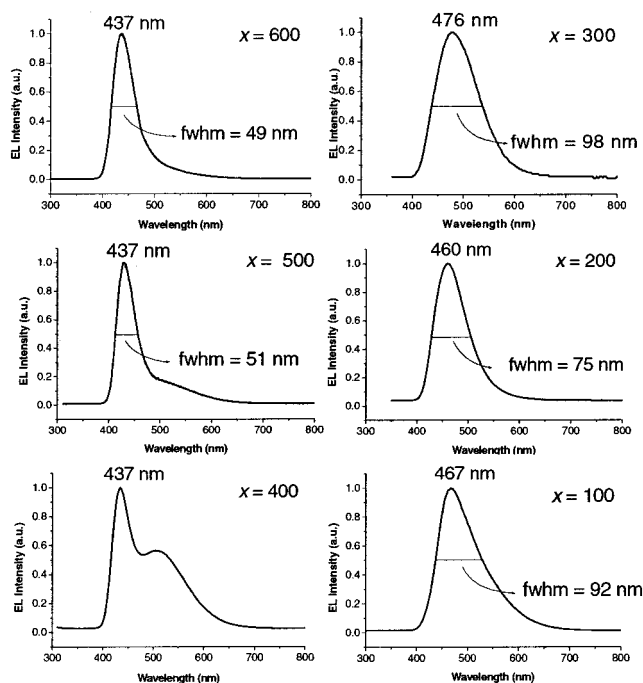


Figure 1. EL spectra of device I's, ITO/NPB (400 Å)/Ph₃Si(PhTPAOXD) (x Å)/Alq₃ (400 Å)/Mg:Ag, where $x = 600, 500, 400, 300, 200,$ and 100 Å and fwhm denotes for full width at half-maximum of marked spectra.

located around 460 nm.¹¹ Thus, the only possibly source for the narrow EL emission band (fwhm ~ 50 nm) with a $\lambda_{\max}^{\text{EL}} \sim 440$ nm is from NPB, the hole-transporting layer of device I.^{12c,15} However, we also notice that a secondary EL emission band located at 490–510 nm of devices with 400 and 500 Å layers of Ph₃Si(PhTPAOXD), and its origin is not apparent to us at this stage of the study. In a comparison of EL of the device with 200 Å layer of Ph₃Si(PhTPAOXD), a broad and red-shifted EL emission band (fwhm = 98 nm) of the device with a 300 Å layer of Ph₃Si(PhTPAOXD) is also hard to explain. Furthermore, the pronounced long-wavelength tailing (which also causes a broad emission band with fwhm = 92 nm) of the $x = 100$ Å device seems to be the EL contribution from green fluorescent Alq₃ ($\lambda_{\max}^{\text{EL}} \sim 520$ nm), an electron-transporting material of device I's. The presence of exciplexes formed by Ph₃Si(PhTPAOXD) and Alq₃ may also contribute to the long-wavelength tailing emission of the spectra. A unified detailed relationship between EL spectra in Figure 1 and layer thickness will be discussed in section G, although some crucial pieces of information are presented here and in the later sections.

One possible reason for the observed EL from Alq₃ is the light emitting from Alq₃ molecules adjacent to the Alq₃-Ph₃Si(PhTPAOXD) interface through Förster energy transfer from Ph₃Si(PhTPAOXD) to Alq₃. To test the efficiency of Förster energy transfer between two molecules, we recorded of the photoluminescence (PL) spectra of the solid film of a mixture of Ph₃Si(PhTPAOXD) and Alq₃ with varied weight ratio (Figure 2). It is noted that the PL spectrum of the sample with 1:1 weight ratio is virtually the same as a pure Alq₃ sample,¹⁶ and the PL emission band from Ph₃Si(PhTPAOXD) is not

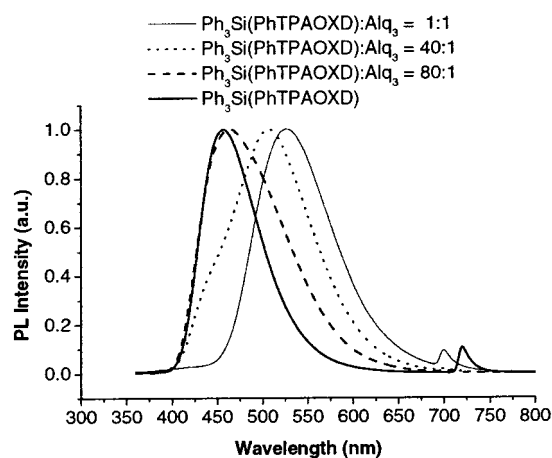


Figure 2. PL spectra of solid films composed of Alq₃ and Ph₃Si(PhTPAOXD). The signals around 700–730 nm are due to the half-frequency of the excitation energy.

discernible until the weight ratio of Ph₃Si(PhTPAOXD) and Alq₃ is greater than 40. This is a clear evidence for an efficient Förster energy transfer from Ph₃Si(PhTPAOXD) to Alq₃. We were somewhat surprised at the result considering the limited spectra overlap between the absorption spectrum ($\lambda_{\max}^{\text{ab}} \sim 390$ nm) of Alq₃ and the emission spectrum of Ph₃Si(PhTPAOXD) ($\lambda_{\max}^{\text{em}} \sim 460$ nm). Furthermore, within the weight ratio we tested, no new emission band was observed in the region with wavelength longer than 550 nm. The emission band of the exciplex formed between Alq₃ and arylamine (part of the Ph₃Si(PhTPAOXD) structure) was known between 550 and 600 nm.¹⁷ Thus, our PL data rule out the possibility of the formation of exciplex at the interface of Alq₃-Ph₃Si(PhTPAOXD). The question of what is the origin of the secondary EL emission band located at 490–510 nm will be answered later on in the following sections

B. Characteristics of Device II. TPBI has been known as an effective electron-transporting material for OLEDs before.^{9c,12c,d,14,15,18} We consider it could be a substitute for Alq₃ here in the device fabrication. Furthermore, since TPBI has an emission band with very short wavelength ($\lambda_{\max}^{\text{em}} < 380$ nm),^{12c} the long-wavelength emission tailing, which we suspect is the EL from Alq₃, of the device I with 100 Å layer of Ph₃Si(PhTPAOXD) may be eliminated if TPBI is replacing Alq₃ in the device. In addition to the optimization of device performance, we fabricated devices ITO/NPB(400 Å)/Ph₃Si(PhTPAOXD)(x Å)/TPBI(400 Å)/Mg:Ag with $x = 100, 200, 300,$ and 400 Å for the verification of our suspicion. The EL spectra of the device containing a layer of Ph₃Si(PhTPAOXD) with different thickness are superimposed in Figure 3. The characteristics of the device performance are also summarized in Table 1. Clearly, the device performance, in all aspects, is worse than those of device I's, indicating the combination of TPBI and Ph₃Si(PhTPAOXD) is not as good as that of Alq₃ and Ph₃Si(PhTPAOXD). However, the data obtained from device II provide valuable information about the secondary EL emission found in device I's (see below).

(15) Tao, Y.-T.; Balasubramaniam, E.; Danel, A.; Jarosz, B.; Tomasik, P. *Appl. Phys. Lett.* **2000**, *77*, 1575.

(16) (a) Kalinowski, J. In *Organic Electroluminescent Materials and Devices*; Miyata, S.; Nalwa, H. S., Eds.; Gordon and Breach: New York, 1997; p 1. (b) van Veldhoven, E.; Zhang, H.; Glasbeek, M. *J. Phys. Chem. A* **2001**, *105*, 1687.

(17) Itano, K.; Ogawa, H.; Shirota, Y. *Appl. Phys. Lett.* **1998**, *72*, 636.

(18) (a) Tao, Y.-T.; Balasubramaniam, E.; Danel, A.; Jarosz, B.; Tomasik, P. *Appl. Phys. Lett.* **2000**, *77*, 1575. (b) Balasubramaniam, E.; Tao, Y.-T.; Danel, A.; Tomasik, P. *Chem. Mater.* **2000**, *12*, 2788. (c) Tao, Y.-T.; Balasubramaniam, E.; Danel, A.; Tomasik, P. *Chem. Mater.* **2001**, *13*, 1207. (d) Chen, B.; Zhang, X. H.; Lin, X. Q.; Kwong, H. L.; Wong, N. B.; Lee, C. S.; Gambling, W. A.; Lee, S. T. *Synth. Met.* **2001**, *118*, 193.

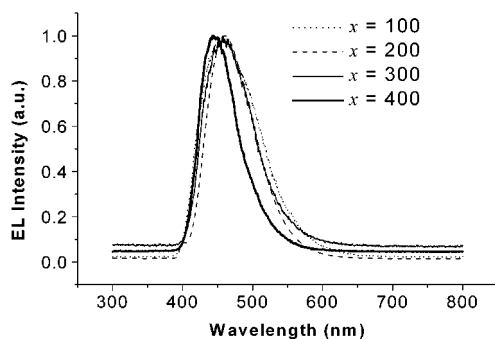


Figure 3. EL spectra of device II's, ITO/NPB(400 Å)/Ph₃Si(PhTPAOXD)-(x Å)/TPBI(400 Å)/Mg:Ag, where $x = 400, 300, 200,$ and 100 Å.

Except for the device with a 400 Å layer of Ph₃Si(PhTPAOXD), all devices show a characteristic EL of Ph₃Si(PhTPAOXD) with $\lambda_{\max}^{\text{EL}}$ at about 460 nm. Once again, EL with $\lambda_{\max}^{\text{EL}}$ at about 440 nm is due to the EL from NPB. The long-wavelength emission tailing observed in the EL of the previous device (device I, $x = 100$ Å) mostly disappears in Figure 3. While the device with a 400 Å layer of Ph₃Si(PhTPAOXD) emits only clean EL spectra of NPB, a shoulder around 490–510 nm was observed for each EL band of the remaining devices. The shoulder of EL spectra is rather similar to the secondary EL emission band observed in device I with 500, 400, and 300 Å layers of Ph₃Si(PhTPAOXD). The experimental finding here strongly implies an exciplex formed by Ph₃Si(PhTPAOXD) and NPB at the interface of the two layers, and the corresponding $\lambda_{\max}^{\text{EL}}$ should be around 490–510 nm.¹⁹

C. Characteristics of Device III. In device II, we replaced the electron-transporting material Alq₃ with TPBI. Unfortunately, our data indicated that the device performance did not improve. In device III, we took an alternative try and we used a different hole-transporting material instead of commonly used NPB for OLEDs. The newly synthesized Ph₂Si(Ph(NPA)₂)₂, a tetraamine species also based on tetraphenylsilane structure, served for this purpose. On the other hand, it will be intriguing to see whether the secondary emission band observed both in devices I and II will be altered or not. If there is difference, we could establish the link between the secondary emission band around 490–510 nm to the exciplex of Ph₃Si(PhTPAOXD) and NPB.

Similar to previously reported Ph₃Si(PhTPAOXD),¹¹ Ph₂Si(Ph(NPA)₂)₂ is also a molecular glass material in the solid state. It is evident that there is no crystalline peak, but only a broad amorphous halo was found on the powder X-ray diffraction (PXRD) spectra (Figure 4). The amorphous property was further confirmed by DSC examination. There are no other signals but a steplike transition on each DSC thermogram of Ph₂Si(Ph(NPA)₂)₂ (Figure 4). This transition was detected around 95 °C on both heating and cooling cycles and was assigned as the T_g of Ph₂Si(Ph(NPA)₂)₂. The glass phase of Ph₂Si(Ph(NPA)₂)₂ is quite stable because of continually showing T_g in every scanning

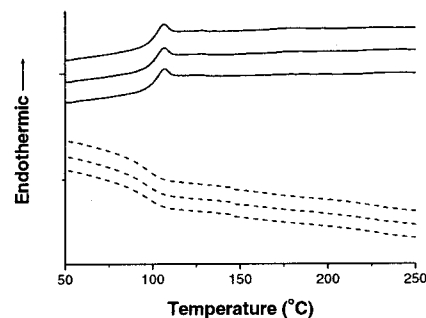
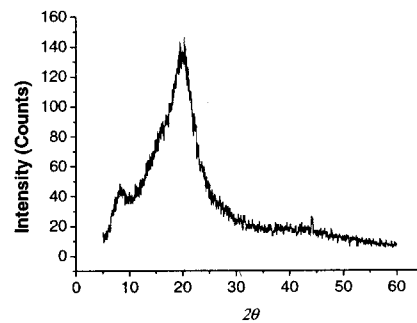


Figure 4. PXRD spectra (top figure) and DSC thermograms (bottom figure) of Ph₂Si(Ph(NPA)₂)₂ with repeated heating (solid lines) and cooling (dashed line) cycles.

cycle of DSC. Similar glass phase stability was reported for Ph₃Si(PhTPAOXD) too.^{11a} We attribute the amorphous property of Ph₂Si(Ph(NPA)₂)₂ to the starburst structure, which is known for an increase in the number of conformers together with nonplanar molecular structure in condense phase.^{13a} Since Alq₃ is known as an amorphous glass material ($T_g > 170$ °C), device III (see below) will be composed of all molecular glass materials with T_g no less than 85 °C.

Accordingly, device III, ITO/Ph₂Si(Ph(NPA)₂)₂ (400 Å)/Ph₃Si(PhTPAOXD) (200 Å)/Alq₃ (400 Å)/Mg:Ag, was fabricated. We used a 200 Å layer of Ph₃Si(PhTPAOXD) in the device to be comparable with the best of device I's. Figure 5 graphically displays the device's characteristics, including I - V - L plots, EL spectrum, external quantum efficiency (QE)- I plot, and CIE 1931 chromaticity diagram. Their corresponding characteristic values are summarized in Table 1. For device III, not only the maximum luminance but also the device's efficiency outweighs those of device I. More importantly, the current density required for maximum luminance is significantly reduced by nearly a factor of 4. In addition, at low current densities 100 and 10 mA/cm² the device shows quite bright EL that almost reaches 6000 and 600 cd/m², respectively, the highest so far. Unfortunately, EL emission band is rather broad (fwhm = 110 nm) and the EL spectrum is red-shifted with $\lambda_{\max}^{\text{EL}}$ at 487 nm. The device now emits light in greenish-blue region as indicated by the high value of coordinates ($x = 0.21, y = 0.33$) on the CIE 1931 chromaticity diagram. In other words, color purity of device III is not as good as that of device I with a 200 or 300 Å layer of Ph₃Si(PhTPAOXD).

It is worth noting that hole-transporting material Ph₂Si(Ph(NPA)₂)₂ significantly reduces the current density of the device but approximately maintains the brightness of the device (Table 1). Therefore, the efficiency of the device is greatly enhanced reaching 3.0%, 3.1 lm/W, or 6.1 cd/A, and these are the highest efficiencies among all devices. On the other hand, the red-shifted EL spectrum also counts for the enhancement of device

(19) To verify the implication here, we prepared a solid film from a mixture of Ph₃Si(PhTPAOXD) and NPB with equal weight ratio and recorded the PL spectra. The PL spectra of pure Ph₃Si(PhTPAOXD) and its 1:1 weight ratio mixture of NPB are nearly superimposable with only a slight mismatch on the long-wavelength side of the spectra.¹¹ This could be a hint for the exciplex formation with $\lambda_{\max}^{\text{EL}}$ at 490–510 nm. Nevertheless, the difference of two spectra is rather small and further evidence is necessary to support the suspected exciplex formation.

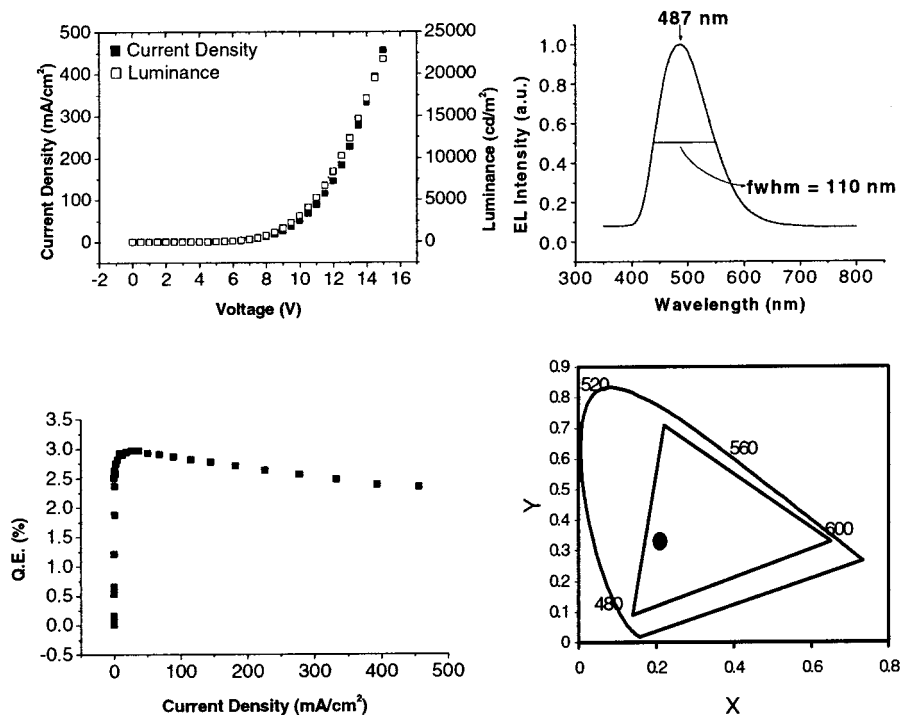


Figure 5. I – V – L characteristics (top left), EL spectra (top right), external quantum efficiency vs current density (bottom left), and CIE 1931 coordinates diagram (bottom right) of device III.

efficiency. A small red shifting of the EL spectrum (a sacrifice on blue color purity) often associates with a better performance of the device. This is important and should be aware for a fair comparison on the performance of blue OLEDs.

Previously unknown $\text{Ph}_2\text{Si}(\text{Ph}(\text{NPA})_2)_2$ has a higher first oxidation potential (0.77 V vs Ag/Ag^+) than that of NPB (0.64 V vs Ag/Ag^+) under CV conditions (Figure 6). This is understandable because π -conjugation between two nearest amino groups of $\text{Ph}_2\text{Si}(\text{Ph}(\text{NPA})_2)_2$ is shorter than that of NPB. In addition, the *meta*-substituted position of $\text{Ph}_2\text{Si}(\text{Ph}(\text{NPA})_2)_2$ limits the conjugated interaction of two amino groups. Corresponding highest occupied molecular orbital (HOMO) energy levels of two compounds can be calculated from CV data. Taking the literature value of ionization potential (IP) 4.8 eV for ferrocene²⁰ and 0.36 V against Ag/Ag^+ for Fc/Fc^+ in our CV measurement, the HOMO energy level is about 5.2 eV for $\text{Ph}_2\text{Si}(\text{Ph}(\text{NPA})_2)_2$ and 5.1 eV for NPB. Therefore, $\text{Ph}_2\text{Si}(\text{Ph}(\text{NPA})_2)_2$ has a closer HOMO energy level than NPB to that of $\text{Ph}_3\text{Si}(\text{PhTPAOXD})$ (~ 5.4 eV), indicating the emissive light from the exciplex in both cases should be somewhat different in energy. If there is an exciplex formation, device III and device I with 200 Å layer of $\text{Ph}_3\text{Si}(\text{PhTPAOXD})$ should show different EL spectra in either $\lambda_{\text{max}}^{\text{EL}}$ or bandwidth of the emission band. This conjecture in fact is consistent with different EL spectra of both devices (Figures 1 and 5). We consider this could be one supporting evidence in addition to the EL spectra shown in Figure 3 and slightly mismatched PL spectra as the indication of the exciplex formed between NPB and $\text{Ph}_3\text{Si}(\text{PhTPAOXD})$.

D. Characteristics of Device IV. The high-performance but unsatisfactory blue color purity of device III inspired us to fabricate the quadruple layer device IV ITO/ $\text{Ph}_2\text{Si}(\text{Ph}(\text{NPA})_2)_2$ (400 Å)/NPB (50 Å)/ $\text{Ph}_3\text{Si}(\text{PhTPAOXD})$ (200 Å)/ Alq_3 (400 Å)/

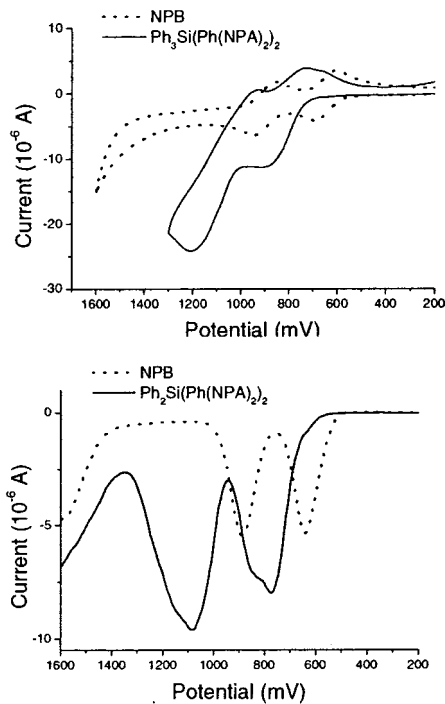


Figure 6. Cyclic voltammograms (top) and Osteryoung square wave voltammograms (bottom) of $\text{Ph}_2\text{Si}(\text{Ph}(\text{NPA})_2)_2$ and NPB in deoxygenated CH_2Cl_2 containing 0.1 M tetrabutylammonium phosphate at 25 °C. All potentials are in volts versus Ag/AgNO_3 (0.01 M in CH_3CN ; scan rate 100 mV s^{-1}).

$\text{Mg}:\text{Ag}$. The rationale of the device configuration is based on the following argument. $\text{Ph}_2\text{Si}(\text{Ph}(\text{NPA})_2)_2$ seems to be particularly useful in reducing the current density and hence enhancing efficiency of the device but adversely seems to form exciplex more readily than NPB does. To take advantage of both materials, both $\text{Ph}_2\text{Si}(\text{Ph}(\text{NPA})_2)_2$ and NPB were used to form a bilayer structure of the hole-transporting material in

(20) Pommerehne, J.; Vestweber, H.; Guss, W.; Mahrt, R. F.; Bäessler, H.; Porsch, M.; Daub, J. *Adv. Mater.* **1995**, *7*, 551.

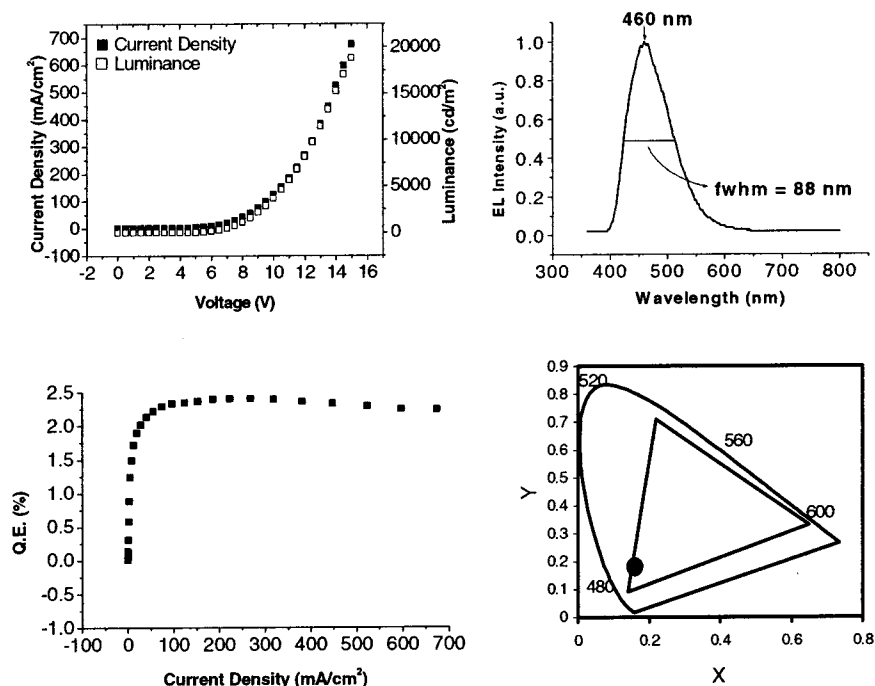


Figure 7. I – V – L characteristics (top left), EL spectra (top right), external quantum efficiency vs current density (bottom left), and CIE 1931 coordinates diagram (bottom right) of device IV.

device IV. The device has a thin layer of NPB (50 Å) sandwiched between $\text{Ph}_2\text{Si}(\text{Ph}(\text{NPA})_2)_2$ and $\text{Ph}_3\text{Si}(\text{PhTPAOXD})$ to preclude direct contact of both materials and hence their exciplex formation. It turns out that device IV is the best device on overall performance including blue EL color purity. Figure 7 graphically shows the characteristics of the device and the values of the corresponding performance are summarized in Table 1. The merit of device IV is its blue color purity ($x = 0.16$, $y = 0.18$) in addition to the low current density (674 mA/cm²) at maximum luminance (18 813 cd/m²) and bright luminance near 3000 cd/m² and over 200 cd/m² at low current densities of 100 and 10 mA/cm², respectively (Table 1). Device IV's efficiency (2.4%, 1.1 lm/W, or 3.1 cd/A) is significantly higher than the remaining devices with comparable blue color purity.

What makes $\text{Ph}_2\text{Si}(\text{Ph}(\text{NPA})_2)_2$ special in enhancing the performance of OLED, particularly in reducing current density and enhancing efficiency of the device? We calculated the LUMO energy level from the HOMO energy (obtained from CV data in section C) and the optical band gap estimated from the absorption onset.^{13d,21} The energy level alignments for device IV are shown in Figure 8.²² Since the energy levels of the LUMO of $\text{Ph}_2\text{Si}(\text{Ph}(\text{NPA})_2)_2$ and NPB are virtually same, it is unlikely that difference in electron-blocking ability of two materials is significant. Therefore, we feel that one of the

possible answers to the question is probably the charge mobility (either hole or electron) of $\text{Ph}_2\text{Si}(\text{Ph}(\text{NPA})_2)_2$, which is rather different from that of NPB. However, this requires charge-mobility measurement to evidence our thoughts.

E. Characteristics of Device V. In this device, we use LiF/Al as cathode material that has been reported for its high efficiencies for OLEDs recently.²³ In addition, CuPc on ITO was known for improving the hole-injection efficiency of OLEDs.²⁴ Therefore, we feel that adopting both LiF/Al and CuPc in the fabrication of blue OLED based on $\text{Ph}_3\text{Si}(\text{PhTPAOXD})$ should provides us devices with higher performance on stability and efficiency. Device V, ITO/CuPc(125 Å)/NPB(400 Å)/ $\text{Ph}_3\text{Si}(\text{PhTPAOXD})$ (200 Å)/Alq₃(400 Å)/LiF(10 Å)/Al, was fabricated accordingly.

One noticeable difference of I – V – L characteristics of the device is that the current density is significantly lower than the other devices in this report. This device showed maximum luminance of 10 260 cd/m² requiring current density only about 277 mA/cm², although at relatively high driving voltage of 17 V (Table 1). The high voltage may be attributed to the thicker layer (10 Å) of LiF than normal (<5 Å). As expected, the photometric efficiency (3.9 cd/A) of device V is one of the highest among all devices (Table 1). However, device V has relatively low power efficiency (1.1 lm/W), which may be attributed to the high driving voltage of the device, which in turn is because of the thick layer of LiF. Device V shows relatively low luminance intensity and may be due to the lower emission intensity of the exciplex, which is now the main emission of the device (Figure 9), compared to $\text{Ph}_3\text{Si}(\text{PhTPAOXD})$. Due to the overall red-shifted EL spectra, the blue color purity of the device is not satisfactory, giving

(21) (a) Thelakkat, M.; Schmidt, H.-W. *Adv. Mater.* **1998**, *10*, 219. (b) Janietz, S.; Bradley, D. D. C.; Grell, M.; Giebeler, C.; Inbasekaran, M.; Woo, E. P. *Appl. Phys. Lett.* **1998**, *73*, 2453. (c) Thomas, K. R. J.; Lin, J. T.; Tao, Y.-T.; Ko, C.-W. *J. Am. Chem. Soc.* **2001**, *123*, 9404. (d) Rajagopal, A.; Wu, C. I.; Kan, A. *J. Appl. Phys.* **1998**, *83*, 2649.

(22) There is a inconsistency of the HOMO energy level of NPB (–5.1 eV) with literature value –5.7 eV.^{13c,21d} This inconsistency may be rationalized by the difference of states (solution vs solid state) of the samples in measurement (CV vs UPS). However, this will not affect the relative position of HOMO energy levels of $\text{Ph}_2\text{Si}(\text{Ph}(\text{NPA})_2)_2$, $\text{Ph}_3\text{Si}(\text{PhTPAOXD})$, and NPB. These levels will shift equally with the same ionization potential of 0.6 eV. The relative position of LUMO energy levels will not be affected either, because the energy gaps between HOMO and LUMO levels were all estimated from the solution absorption spectra.

(23) (a) Hung, L. S.; Tang, C. W.; Manson, M. G. *Appl. Phys. Lett.* **1997**, *70*, 152. (b) Heil, H.; Steiger, J.; Karg, S.; Gastel, M.; Ortner, H.; von Seggern, H.; Stössel, M. *J. Appl. Phys.* **2001**, *89*, 420 and references therein.

(24) Van Slyke, S. A.; Chen, C. H.; Tang, C. W. *Appl. Phys. Lett.* **1996**, *69*, 2160.

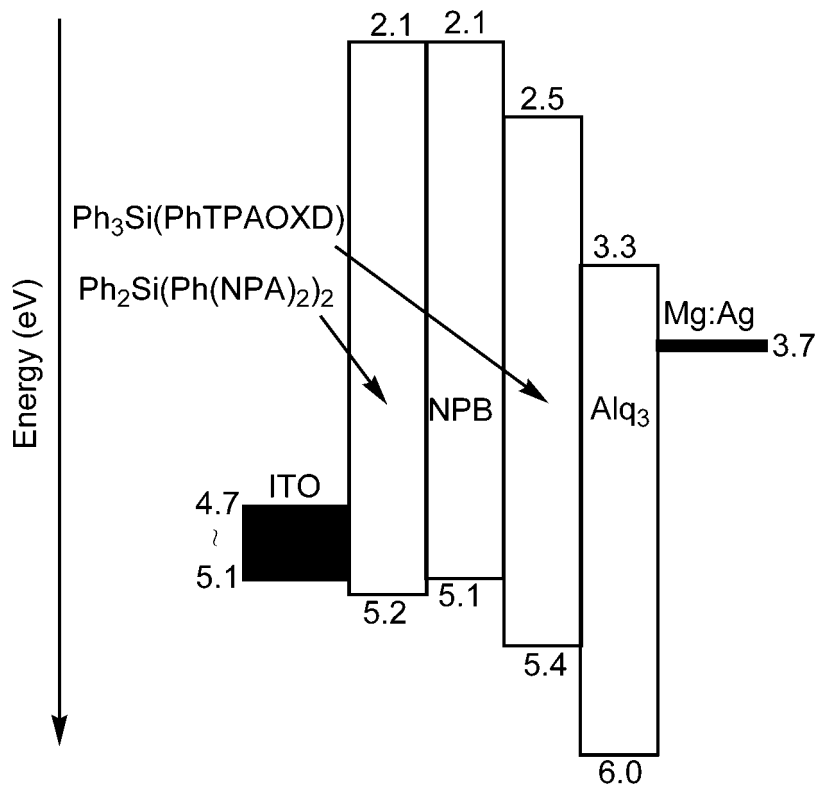


Figure 8. Relative energy level diagram for device IV.

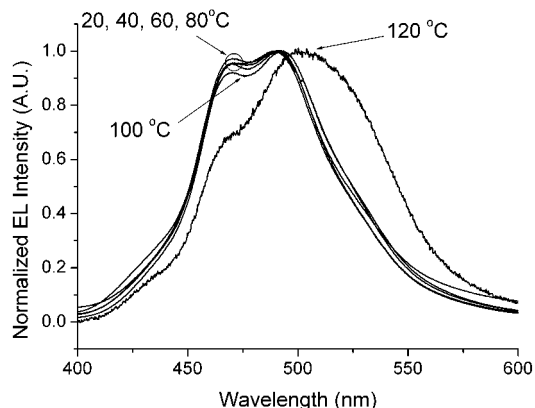


Figure 9. EL spectra of device V at room temperature (20 °C) and after heating at elevated temperatures (40, 60, 80, 100, and 120 °C) for 20 min.

coordinates ($x = 0.15$, $y = 0.26$) on the CIE 1931 chromaticity diagram (Table 1).

Nevertheless, EL spectra of device V reveal a new interesting profile (Figure 9). Beside the emission bands at 460 nm of $\text{Ph}_3\text{Si}(\text{PhTPAOXD})$ and 440 nm of NPB, emission bands due to the exciplex of NPB– $\text{Ph}_3\text{Si}(\text{PhTPAOXD})$ ($\lambda_{\text{max}}^{\text{EL}}$ at ~ 490 nm), and Alq_3 ($\lambda_{\text{max}}^{\text{EL}}$ at ~ 520 nm) can all be identified on the EL spectra. Furthermore, $\lambda_{\text{max}}^{\text{EL}}$ of the whole spectra of device V is centered around 489 nm, which is about the location of the exciplex emission. Since device V without CuPc shows a similar EL spectra profile, we attribute the profile of EL spectra to the different cathode material (LiF/Al instead of MgAg).

F. Temperature Stability Studies of Device V. The temperature stability of device V was examined by annealing studies to evaluate the thermal stability of these OLEDs. The encapsulated device was heated from room temperature (20 °C) to elevated temperatures 40, 60, 80, 100, and 120 °C sequentially.

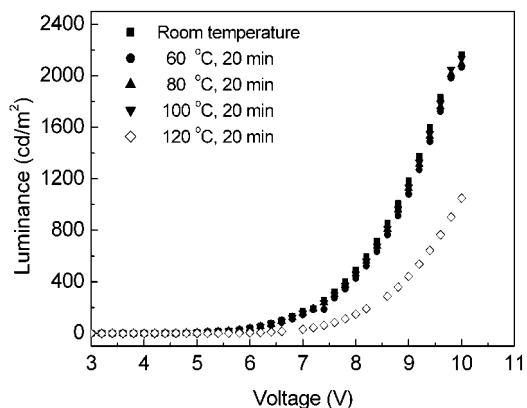


Figure 10. Temperature dependence of luminance vs voltage of device V.

Desired measurements were performed right after the device was held at the desired temperature for 15–20 min. The luminance versus voltage (Figure 10) as well as EL spectra of the device (Figure 9) at these five temperatures was recorded. From Figure 10, it is evident that the brightness of the device is hardly changed at temperatures 20, 40, 60, 80, and 100 °C but drops dramatically at temperature 120 °C. Similar temperature dependence is observed for EL spectra (Figure 9), because there is virtually no change in spectra of the devices heated below 80 °C. Minute spectral change, a slight weakening of the emission band of $\text{Ph}_3\text{Si}(\text{PhTPAOXD})$ that has no effect on overall luminance, becomes discernible at 100 °C (Figure 9). Once again, major spectral change is not found until the device is heated at 120 °C. The fact that the EL spectra have a minor change between 80 and 100 °C, but a major change between 100 and 120 °C is consistent with T_g of $\text{Ph}_3\text{Si}(\text{PhTPAOXD})$ and NPB. Massive exciplex formation, initiated by the interface-

crossing diffusion of both $\text{Ph}_3\text{Si}(\text{PhTPAOXD})$ and NPB, does not occur until temperatures higher than T_g of both materials, 85 and 100 °C for $\text{Ph}_3\text{Si}(\text{PhTPAOXD})$ and NPB,^{11a,13d} respectively.

However, we believe that molecules in either reduced or oxidized form in OLED in addition to close contact are necessary for exciplex formation. This is because we did not observe PL spectral difference between thin solid films of the mixture (1:1 weight ratio) of $\text{Ph}_3\text{Si}(\text{PhTPAOXD})$ and NPB before and after heating at 120 °C. The EL changes of device V annealed at 120 °C must be related to the charges (electron and hole) that are injected onto the molecular materials. The charged molecular materials are readily interactive to form exciplexes because of the close proximity of different molecules after the thermal diffusion.

Relevantly, the device's EL spectra basically remain unchanged (even under heating condition) when the driving voltage is less than about 10 V (Figures 9 and 10), indicating a reasonable voltage stability of the device. However, devices do show altered EL spectra with weakening, broadening, and red-shifted spectral profile under high driving voltage (12–16 V). The spectra are not recoverable when devices are back down to low voltage. This observation is not only limited to device V but a general phenomenon for the remaining devices I–IV. Since high voltage comes with high current density and which in turn generates joule heating, we believe that device decay is due to the adverse exciplex formation following a similar mechanism mentioned above.

Device failure observed here because of the thermal expansion of the organic–organic interface associated with low- T_g materials has not attracted much attention but is as crucial as the crystallization issue of OLEDs built on molecular materials.²⁵

Regarding the issue of exciplex formation, it is interesting to find that the EL spectra of device V heated at 120 °C show a broad spectrum with $\lambda_{\text{max}}^{\text{EL}}$ between 490 and 510 nm, similar to that of the emission band of NPB– $\text{Ph}_3\text{Si}(\text{PhTPAOXD})$ exciplex.²⁶ The results shown here not only confirm the exciplex formation proposed earlier but also provide an insightful understanding of possible failure mechanisms of the OLED device based on molecular materials.

G. Thickness (of Light-Emitting Layer) Dependence of EL Spectra of Device I. The variation of EL spectra shown in Figure 1 was hard to rationalize in the early stage of this study. With fruitful data accumulated so far, we are now ready to have a full explanation of the changing spectra. It has been previously reported that structure moiety of diphenylamino-substituted oxadiazole is hole-blocking in nature.^{12d} Therefore, a thick layer (600 Å) of $\text{Ph}_3\text{Si}(\text{PhTPAOXD})$ in device I will confine the charge-recombination zone within the layer of NPB, and hence, a clean EL spectrum ($\lambda_{\text{max}}^{\text{EL}}$ at 437 nm) of NPB is observed. When the thickness of the light-emitting layer $\text{Ph}_3\text{Si}(\text{PhTPAOXD})$ is changed, the charge-recombination zone of the device is simultaneously altered. The area covered by the zone is changed and possibly the zone width is also varied, since the charge

(either hole or electron) mobility of the multilayer device is changed by the different thickness of the $\text{Ph}_3\text{Si}(\text{PhTPAOXD})$ layer. While the layer of $\text{Ph}_3\text{Si}(\text{PhTPAOXD})$ becomes thinner (500 and 400 Å), the charge-recombination zone shifts closer to the center of the device, covering part of the NPB and $\text{Ph}_3\text{Si}(\text{PhTPAOXD})$ layers containing the interface area (area of exciplex formation) in between. EL from $\text{Ph}_3\text{Si}(\text{PhTPAOXD})$ and its exciplex with NPB becomes more and more pronounced, although EL of NPB is still the major feature. The broad EL spectrum of device I with a 300 Å layer of $\text{Ph}_3\text{Si}(\text{PhTPAOXD})$ is composed of mainly of the EL from $\text{Ph}_3\text{Si}(\text{PhTPAOXD})$ accompanied with substantial EL from exciplex and a small amount of EL from NPB, respectively. All three components merge into one unresolved broad EL spectrum with $\lambda_{\text{max}}^{\text{EL}}$ at 476 nm. The charge-recombination zone of the device with a 200 Å layer of $\text{Ph}_3\text{Si}(\text{PhTPAOXD})$ just locates inside the blue light-emitting layer perfectly without touching the interface area on either side of the layer. This is based on the fact that almost the same EL ($\lambda_{\text{max}}^{\text{EL}}$ at 460 nm, fwhm = 75 nm) and PL ($\lambda_{\text{max}}^{\text{EL}}$ at 457 nm, fwhm = 75 nm) spectra of the device were observed.¹¹ When the layer of $\text{Ph}_3\text{Si}(\text{PhTPAOXD})$ is further decreased to 100 Å thick, the EL spectrum becomes broad again with tailing on the long-wavelength side. Here, the charge-recombination zone of the device may reach the Alq_3 layer, or maybe the width of zone is too wide too to be accommodated totally inside $\text{Ph}_3\text{Si}(\text{PhTPAOXD})$ layer (now only 100 Å thick). Therefore, some of the EL from the exciplex may reoccur back in the spectra. On the other hand, the charge-recombination zone maybe close enough to the interface of $\text{Ph}_3\text{Si}(\text{PhTPAOXD})$ and Alq_3 , and Förster energy transfer between two materials adjacent to the interface becomes possible.

Summary

Blue light-emitting OLEDs with good color chromaticity, high luminance, and respectable efficiency have been achieved. Performance of blue OLEDs based on an amorphous molecular material, $\text{Ph}_3\text{Si}(\text{PhTPAOXD})$, is highly sensitive to light-emitting layer thickness, hole blocking material, hole transporting material, and cathode materials. The shifting of charge recombination zone (and maybe the difference of the zone width) is proposed to be the reason for the variation of EL spectra when the thickness of light-emitting layer is changed. Exciplex formation, between the hole transporting material (NPB) and blue light-emitting material ($\text{Ph}_3\text{Si}(\text{PhTPAOXD})$), is verified in this study. The emissive light ($\lambda_{\text{max}}^{\text{EL}}$ at 490–510 nm) from the annoying exciplex can be successfully avoided in device I by limiting the charge recombination zone inside light-emitting layer through layer thickness control.

The blue OLED reported here has been examined for temperature stability and shows stable luminance within a temperature range of room temperature to 100 °C. Major loss on luminance was detected at temperature above 100 °C, which is accordant with the T_g values of NPB. The weakening of luminance at elevated temperature is attributed to the exciplexes, which form easily under the charge injection in addition to the close contact due to the thermal diffusion of materials at temperatures above T_g . The OLED temperature stability studies in this report reveal and prove one failure mechanism, which is associated with molecular diffusion and should be considered

(25) Fenter, P.; Schreiber, F.; Bulovic, V.; Forrest, S. R. *Chem. Phys. Lett.* **1997**, *277*, 521.

(26) For device V, part of the reason for the broad EL spectrum at 120 °C in Figure 9 may be due to the enhanced EL contribution from Alq_3 . The EL contribution from Alq_3 also causes a red-shifted $\lambda_{\text{max}}^{\text{EL}}$ compared to that of spectra at lower temperatures.

as one of the key issues in searching for molecular material-based OLEDs with long stability.

Acknowledgment. We thank Academia Sinica and the China Petroleum Cooperation of ROC for supporting this work. Helpful assistance in the fabrication and measurement of the OLED devices from Dr. Chung-Wen Ko and Prof. Yu-tai Tao are also acknowledged.

Supporting Information Available: CIE 1931 chromaticity diagram of device I's, $I-V-L$ characteristics and efficiency vs current density plots of device V, and PL spectra of solid films composed of NPB and Ph₃Si(PhTPAOXD) (PDF). This material is available free of charge via the Internet at <http://pubs.acs.org>.

JA0255150